Defence Science Journal, Vol. 67, No. 1, January 2017, pp. 108-118, DOI : 10.14429/dsj.67.9236

A Singular Perturbation based Midcourse Guidance Law for Realistic Air-to-air Engagement

M. Manickavasagam[*], A.K. Sarkar[#], and V. Vaithiyanathan[@]

[*]*Advance System Laboratory, Kanchanbagh, Hyderabad - 500 058, India*
[#]*Defence Research and Development Laboratory, Kanchanbagh, Hyderabad - 500 058, India*
[@]*SASTRA University, Thanjavur - 613 401, India*
[*]*E-mail: manick65@yahoo.com,*

ABSTRACT

In this study, a singular perturbation based technique is used for synthesis and analysis of a near optimal midcourse guidance law for realistic air-to-air engagement. After designing the proposed midcourse guidance law using three dimensional point mass formulation it has been validated through detailed realistic six degrees of freedom simulation. During terminal phase only proportional navigation guidance have been used. The calculation of optimal altitude in present guidance law has been carried out using Newton's method, which needs generally one iteration for convergence and suitable for real-time implementation. Extended Kalman filter based estimator has been used for obtaining evader kinetic information from both radar and seeker noisy measurements available during midcourse and terminal guidance. The data link look angle constraint due to hardware limitation which affects the performance of midcourse guidance has also been incorporated in guidance law design. Robustness of complete simulation has been carried out through Monte Carlo studies. Extension of launch boundary due to singular perturbation over proportional navigation guidance at a given altitude for a typical engagement has also been reported.

Keywords: Singular perturbation; Midcourse guidance law; Beyond visual range; Interceptor

NOMANCLATURE

BVR	Beyond visual range
DCM	Direction cosine matrix
CDF	Cumulative distribution frequency
CG	Centre of gravity
DOF	Degree of freedom
EKF	Extended Kalman filter
GBPN	G-biased proportional navigation
LOS	Line of Sight
LV	Local vertical
MC	Monte Carlo simulation
MMI	Mass moment of Inertia
ND	Normal distribution
PIP	Predicted impact point
PN	Proportional navigation
SDINS	Strap down inertial navigation system
SP	Singular perturbation guidance law
TPBVP	Two point boundary value problem
UD	Uniform distribution

1. INTRODUCTION

In air-to-air engagement, it is desirable to launch an interceptor (pursuer) against a target (evader) when it is beyond visual range (BVR) of the pilot of the launch aircraft. The evader is tracked by on-board radar and the information is communicated from launch aircraft to the pursuer through a data link. During the midcourse phase of flight, the objective of the guidance system is to reduce the line-of-sight (LOS) separation between the pursuer and evader and to place it within the seeker lock-on range. Classical guidance laws like proportional navigation (PN) perform well for short and medium range application. The aim of the present investigation is to study the singular perturbation (SP) based guidance law as a viable alternate to the conventional guidance laws for midcourse application in a realistic pursuer evader air-to-air engagement. The SP approach gives real time approximate solution to optimal control problem and eliminates the need for extensive computations[1]. An excellent historical review of SP theory as it has developed over the years was discussed by Naidu and Calise[2] and O'malley[3]. The paper on SP-based guidance to minimise the miss distance in real time for short range air-to-air interception, by Sridhar and Gupta[4] reported that it provides a significant improvement over PN. Calise[5] has used SP method for on-line optimal control of an aircraft as a minimum time interception problem. Later, by applying the same technique for BVR interception, Cheng and Gupta[6], Sheu[7], *et al.* and Weston[8], *et al.* have reported that by proper trajectory shaping during midcourse, almost 25 per cent increase in effective launch range over PN guidance could be achieved, Subsequently, Menon and Briggs[9], Kee[10], *et al.* and Raikwar[11], *et al.* reported the superior performance of near optimal SP guidance law over PN. Sigal and Ben-Asher[12] computed SP based midcourse guidance command and optimum initiation time of second pulse of a tactical flight vehicle (FV) with pulse rocket motor. Chandrakant[13] has designed midcourse guidance

Received : 15 September 2015, Revised : 29 August 2016
Accepted : 19 October 2016, Online published : 22 December 2016

law of an air to surface FV. Here the path constraints have been accounted for by constructing the optimal altitude in the outer layer solution. The boundary layer correction on fast variable also have been done using feedback linearisation.

In all the above cited references the SP guidance law has been developed by optimising different performance indices using three degrees of freedom (3 DOF) point mass model of pursuer and evader. But the intricacies of implementation of SP guidance law in realistic six degree of freedom (6 DOF) simulation model along with detailed results are not reported. This study bridges this gap by addressing several of these practical issues. The paper's contributions are :

(i) Revisit of SP guidance law derivation along with algorithmic details as extension of[6,11]

(ii) A novel real time implementable algorithm for computing optimum altitude, critical for a successful on-board implementation of the SP guidance

(iii) Several implementation issues for realistic 6 DOF simulation with SP guidance law and

(iv) Pursuer has to always within the maximum beam width $(\pm 20^{0})$ of the data link of the launch aircraft (Fig. 1).

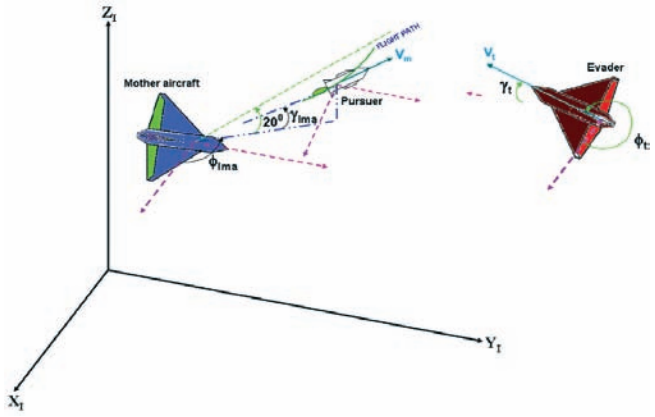

Figure 1. Air-to-air engagement (pursuer, evader and launch aircraft).

This important practical constraint has also been modelled in the present problem. The noisy radar measurements from launch aircraft radar during midcourse phase has been processed by extended kalman filter (EKF) based estimator in closed loop to estimate its current position and velocity components. This Kinetic information is communicated to the pursuer from launch aircraft through this data link and it form the inputs to the midcourse guidance algorithm to generate its lateral acceleration (latax) demand along the yaw and pitch planes. Robustness of the proposed midcourse guidance algorithm has been shown against different system uncertainties and sensor noise variation through large number of Monte Carlo (MC) runs.

2. DERIVATION OF SP GUIDANCE LAW

The governing equations of motion of pursuer as 3D point mass model assuming flat earth is (Fig. 2)

$$\dot{x} = f_1(\bar{x},\bar{u}) = V\cos\gamma\cos\phi \;\; ; \; x(t_0) = x_0$$

$$\dot{y} = f_2(\bar{x},\bar{u}) = V\cos\gamma\sin\phi \;\; ; \;\; y(t_0) = y_0$$

$$\dot{h} = f_3(\bar{x},\bar{u}) = V\sin\gamma \;\;\;\;\;\; ; \;\; h(t_0) = h_0$$

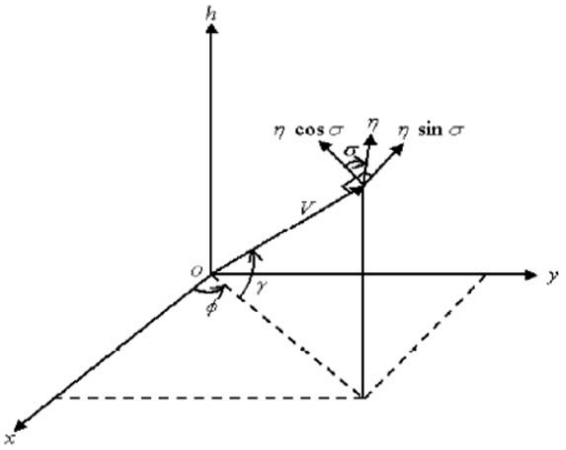

Figure 2. Pursuer configuration in state space for SP guidance law.

$$\dot{E} = f_4(\bar{x},\bar{u}) = \frac{V(T-D)}{mg} \;\; ; \;\; E(t_0) = E_0 \tag{1}$$

$$\dot{\phi} = f_5(\bar{x},\bar{u}) = \frac{g\eta\sin\sigma}{V\cos\gamma} \;\; ; \;\; \phi(t_0) = \phi_{t0}$$

$$\dot{\gamma} = f_6(\bar{x},\bar{u}) = \frac{g(\eta\cos\sigma - \cos\gamma)}{V} \;\; ; \; \gamma(t_0) = \gamma_{t0}$$

The state variables (x,y,z) are downrange, cross range and altitude of the pursuer in the inertial frame, $E = \left(V^2/(2g) + h\right)$ is the specific range, V is pursuer velocity, γ is the flight path angle, ϕ is the heading angle, T is the thrust, D is the drag experienced by the pursuer, m is the purser mass, g is acceleration due to gravity, η is the total load factor and σ is the orientation of the load factor (bank angle). The control variables $\bar{u}$ are (η,σ). Now let us define the load factor as

$$\eta = \frac{L}{W} = \frac{L}{mg} \tag{2}$$

where L is the lift and W is pursuer weight. At any instant of time V should be interpreted as

$$V = \sqrt{2g\left(E-h\right)} \tag{3}$$

In the present analysis the aerodynamic drag is calculated as follow:

$$D = D_0 + D_i\eta^2;\; D_0 = C_{D0}QS;$$

$$D_i = \frac{m^2g^2k_d}{QS};\; Q = \frac{1}{2}\rho V^2;\; k_d = \frac{1}{C_{N\alpha}} \tag{4}$$

Here k_d and C_{D0} are functions of Mach number M and ρ is function of altitude h.

$$k_d = k_d(M);\; C_{D0} = C_{D0}(M,h);\; \rho = \rho(h) \tag{5}$$

The in-flight evader state is used instead to predict the point of interception (PIP) which is treated as a terminal condition for the system of Eqn (1). The terminal conditions.

$$(x,y,h)\;(t_f) = (x_f, y_f, h_f) \tag{6}$$

2.1 Optimal Control Formulation of SP Guidance

The performance index for optimal guidance problem to be analysed is

$$\text{Minimise} \;\; J = \int_{t_0}^{t_f}(1+k\eta^2)dt \tag{7}$$

where $(t_0,\ t_f)$ are initial and final time, η is the resultant

load factor and k ($0 \le k \le 1$) is the weighting factor. Also the guidance solution should satisfy the following inequality constraints.

$$|\eta| \le \eta_{\max} \text{ and } h \le h_{\max} \tag{8}$$

where $\eta_{\max}$ is the maximum allowable load factor on the pursuer and $h_{\max}$ is the maximum height of the pursuer so that its LOS wrt launch aircraft should be less than the maximum solid angle of the data link ($\pm 20^0$).

Solution to the optimal control problem can be obtained by defining a Hamiltonian[1] as

$$H = \lambda_\xi^T \dot{\xi} + (1 + k\eta^2) = \lambda_\xi^T f(x,u,t) + (1 + k\eta^2) \tag{9}$$

where $\xi = (x, y, h, E, \phi, \gamma)^T$ and $\lambda_\xi = (\lambda_x, \lambda_y, \lambda_z, \lambda_x, \lambda_x, \lambda_x, \lambda_x,)^T$. Here λ_ξ elements are Lagrange multipliers which satisfy

$$\dot{\lambda}_\xi = -\left(\frac{\partial H}{\partial \xi}\right)^T$$
$$\lambda_\xi(t_f) = \left(x_f - x, y_f - y, z_f - z, 0, 0, 0\right)^T \tag{10}$$

λ_x and λ_y are constraints since *H* does not depend explicitly on x and y. the optimality conditions are

$$\frac{\partial \mathrm{H}}{\partial \eta} = 0; \frac{\partial \mathrm{H}}{\partial \sigma} = 0 \tag{11}$$

The transversality condition due to free final time is

$$H\left(t_f\right) = 0 \tag{12}$$

where *H* is time varying. Offline solution of a 12-th order two points boundary value problem (TPBVP) resulting from the above formulation, is not amenable to real time implementation. This facts lead us to other solution methods such as the SP theory based on time scale separation.

2.2 Time-Scale Separation

In SP theory the derivatives of some of the states are multiplied by a small positive scalare[14]

$$\dot{x} = f(x, z, \varepsilon, t),\ x(t_0) = x(0),\ x \in R^n \tag{13}$$

$$\varepsilon \dot{z} = g(x, z, \varepsilon, t),\ z(t_0) = z(0),\ z \in R^m \tag{14}$$

The scalar ϵ is a modelling tool. When we setϵ = 0, the dimension of the state space of Eqns. (13)-(14) reduces from n+m to n because the differential Eqn. (14) consisting of $\varepsilon \dot{z}$ degenerates into algebraic or transcendental equation

$$\varepsilon \dot{z} = 0 = g\left(\hat{x}, \hat{z}, 0, t\right),\ \hat{z} \in R^m \tag{15}$$

In the present problem, there exists a clear separation in time scale among all the state variables which canbe divided into three groups[6,11] such as (i) Slowest: (x, y, E), (ii) Slow: *h*, and (iii) fast: (γ , ϕ). Here at first the slowest variables are solved assuming fast variables to be in equilibrium. Then, the slow variable along with the slowest variable solutions $\left(\hat{x}, \hat{y}, \hat{E}, h\right)$, are solved assuming fast variables be in equilibrium. Finally the last fast variable (γ, ϕ) are solved along with the slowest and slow variables $\left(\hat{x}, \hat{y}, \hat{E}, \hat{h}\right)$. Note that results obtained from each individual layer is not optimal because they do not satisfy the boundary condition imposed in Eqn (6). So an ad hoc boundary layer correction needs to be carried out in $\left(\hat{h}.\hat{\gamma}\right)$ in the second and third layer for adjusting evolved near-optimal altitude and flight path angle to final values as given in Eqn (6).

2.3 Outer Layer Solution

In section 2.2, the overall SP algorithm has been described eliciting the importance of timescale separation. Now let us derive the relevant equation for real time solution of present problem.

2.3.1 Slowest Time Scale

The slowest variable are (x, y, E). Since (h, ϕ, γ) are faster, according to Eqn. (15),

$$\varepsilon \dot{h} = V \sin\gamma = 0;\ \varepsilon \dot{\phi} = \frac{g\eta \sin\sigma}{V \cos\gamma} = 0;\ \varepsilon \dot{\gamma} = \frac{g(\eta \cos\sigma - \cos\gamma)}{V} = 0 \tag{16}$$

So, in the equilibrium condition

$$\gamma_1 = 0 \quad \sigma_1 = 0 \quad \eta_1 = 1 \tag{17}$$

The simplified Hamiltonian Eqn. (9) is then

$$H_1 = \lambda_{x1} V_1 \cos\phi_1 + \lambda_{y1} V_1 \sin\phi_1 + \lambda_{E1} \frac{V_1(T - D_1)}{mg} + 1 + k \tag{18}$$

The subscript '1' denotes the state and control variables in a slow time scale. In this time frame h_1 and ϕ_1 may be considered as pseudo control variables. The optimal value of ϕ_1 is given by

$$\frac{\partial H_1}{\partial \phi_1} = 0;\ \tan\phi_1 = \frac{\lambda_{y1}}{\lambda_{x1}} \tag{19}$$

Since λ_{x1} and λ_{y1} are constants in Eqn. (10), ϕ_1 is also a constant. Now using Eqns. (1) and (6) we get

$$\tan\phi_1 = \frac{\dot{y}_1}{\dot{x}_1} = \frac{(y_f - y_0)/t_{go}}{(x_f - x_0)/t_{go}} = \frac{(y_f - y_0)}{(x_f - x_0)} \tag{20}$$

The transversality condition in Eqn. (12) implies that

$$\lambda_{x1} V_1\left(t_f\right)\cos\phi_1 + \lambda_{y1} V_1\left(t_f\right)\sin\phi_1 + \lambda_{E1} \frac{V_1(t_f)\left(T - D_1\right)}{mg} + 1 + k = 0 \tag{21}$$

Again, based on Eqn. (10),

$$\lambda_{E1}\left(t_f\right) = 0 \tag{22}$$

So using Eqns. (21)-(22) we obtain

$$\lambda_{x1} = -\frac{(1+k)\cos\phi_1}{V_1\left(t_f\right)}\ ;\ \lambda_{y1} = -\frac{(1+k)\sin\phi_1}{V_1\left(t_f\right)} \tag{23}$$

λ_{E1} now can be obtained from Eqns. (21) and (23). But $H_1(t)$ is time varying and not autonomous. To permit $H_1(t) = 0$ the concept of average thrust T_{av} and m_{av} is very crucial[6,9]. Which will be discussed later.

$$H_1(t) = 0\ \lambda_{x1} V_1 \cos\phi_1 + \lambda_{y1} V_1 \sin\phi_1 + \lambda_{E1} \frac{V_1\left(T_{av} - D_1\right)}{m_{av} g} + 1 + k = 0 \tag{24}$$

Using Eqns. (23)-(24), we obtain

$$\lambda_{E1} = \frac{m_{av} g\left(1+k\right)}{T_{av} - D_1}\left\{\frac{1}{V_1\left(t_f\right)} - \frac{1}{V_1}\right\} \tag{25}$$

where $V_1\left(t_f\right)$ is V_1 at the t_f. The pursuer forward acceleration can be approximately written as

$$\dot{V}_1 = \frac{T_{av} - D_1}{m_{av}} = \frac{V_1\left(t_f\right) - V_1}{t_{go}} \tag{26}$$

Based on Eqns. (25)-(26) we can rewrite the expression for λ_{E1} as

$$\lambda_{E1} = -\frac{g(1+k)t_{go}}{V_1 V_1(t_f)} \tag{27}$$

But calculation of λ_{E1} from Eqn. (27) needs time-to-go (t_{go}) estimation which will be discussed later. Final step is the computation of optimal altitude h_1 based on the equation $\frac{\partial H_1}{\partial h_1} = 0$. This yields $\frac{\partial H_1}{\partial h_1} = \frac{g}{V_1}$ and

$$-\lambda_{x1}\frac{g}{V_1}\cos\phi_1 - \lambda_{y1}\frac{g}{V_1}\sin\phi_1 - \lambda_{E1}\frac{(T-D_1)}{mg}\frac{g}{V_1} - \lambda_{E1}\frac{V_1}{mg}\frac{\partial D_1}{\partial h_1} = 0 \tag{28}$$

After eliminating $(\lambda_{x1}, \lambda_{y1})$ based on Eqns. (23) and (28) we obtain

$$\frac{g(1+k)}{V_1(t_f)} - \lambda_{E1}\left(\frac{(T-D_1)}{mg} + \frac{V_1^2}{mg}\frac{\partial D_1}{\partial h_1}\right) = 0 \tag{29}$$

Again, after eliminating λ_{E1} based on Eqns. (27) and (29), we obtain

$$\frac{\partial D_1}{\partial h_1} = -\left(\frac{mV_1}{t_{go}} + (T-D_1)\right)\frac{g}{V_1^2} \tag{30}$$

Equation (30) has to be solved to obtain the optimal *h*. Here $D = D(\rho, V)$ along with $\rho = \rho(h)$ and

$$D = \frac{1}{2}\rho V^2 S(C_{D0} + C_{Di}) = D_0 + D_1\eta^2 = \frac{1}{2}\rho V^2 C_{D0} + \frac{(mg)^2}{\frac{1}{2}\rho V^2 C_{N\alpha}}\eta^2$$

and $\frac{\partial V}{\partial h} = -\frac{g}{V}$ $\frac{\partial D_0}{\partial h} = \frac{1}{2}SC_{D0}\left(V^2\frac{\partial\rho}{\partial h} - 2\rho g\right)$ and

$$\frac{\partial D_i}{\partial h} = (mg)^2\frac{(1/C_{N\alpha})}{(S/2)}\frac{V^2\frac{\partial\rho}{\partial h} - 2\rho g}{(\rho V^2)^2} \tag{31}$$

$$\frac{\partial D}{\partial h} = \frac{\partial D_0}{\partial h} + \frac{\partial D_i}{\partial h}\eta^2 = \frac{\partial D_0}{\partial\rho}\frac{\partial\rho}{\partial h} + \frac{\partial D_0}{\partial V}\frac{\partial V}{\partial h} + \frac{\partial D_i}{\partial\rho}\frac{\partial\rho}{\partial h}\eta^2 + \frac{\partial D_i}{\partial V}\frac{\partial V}{\partial h}\eta^2$$

$$= \frac{1}{2}SC_{D0}\left(V^2\frac{\partial\rho}{\partial h} - 2\rho g\right) - \left\{(\eta mg)^2\frac{(1/C_{N\alpha})}{(S/2)}\frac{V^2\frac{\partial\rho}{\partial h} - 2\rho g}{(\rho V^2)^2}\right\}$$

The optimal height h_1 can be obtained by optimising the cost function based on Eqn. (30).

$$J_h(h_1) = \left[\frac{\partial D_1}{\partial h_1} + \left\{\frac{m_{av}V_1}{t_{go}} + (T_{av} - D_1)\right\}\frac{g}{V_1^2}\right]^2 \tag{32}$$

where, $\frac{\partial D_1}{\partial h_1}$ is obtained from Eqn. (31). Cost function Eqn. (32) is optimised to obtain h_1 using Newton method.

$$\hat{h}_{1,k+1} = \hat{h}_{1,k} - \left[\left(\nabla^2 J_h\right)_k\right]^{-1}(\nabla J_h)_k \tag{33}$$

Change and Gupta[6] as well as Raikwar[11], *et al.* used approximate algorithm for calculation of optimal h_1. Present algorithm is computationally slightly more complex but more accurate. Initial guess altitude h_1 is supplied as input. Subsequently, h_1 obtain from the previous guidance step is used as initial guess for current guidance computation step. For satisfying the inequality constraint as given in Eqn. (8), h_1 is considered by $h_{\max}$. Then, for current (h, V) of pursuer, V_1 at altitude h_1 may be obtained from specific energy conservation relation

$$\frac{V_1^2}{2g} + h_1 = \frac{V^2}{2g} + h \tag{34}$$

2.3.2 Slow Time Scale

The slow time scale is defined by the altitude (*h*) dynamics which is faster than the dynamics of $(x, y.E)$ but slower than (γ, ϕ). To solve for the altitude dynamics $(\lambda_{x1}, \lambda_{y1}, \lambda_{E1})$ from the slowest time scale are used. Since (ϕ, γ) are faster than *h* can be assumed in equilibrium

$$\varepsilon\dot{\phi} = \frac{g\eta\sin\sigma}{V\cos\gamma} = 0\ ;\ \varepsilon\dot{\gamma} = \frac{g(\eta\cos\sigma - \cos\gamma)}{V} = 0 \tag{35}$$

$$\sigma_2 = 0 \quad \eta_2 = \cos\gamma_2$$

The simplified Hamiltonian Eqn. (9) in the present context is

$$H_2 = \lambda_{x1}V_2\cos\gamma_2\cos\phi_1 + \lambda_{y1}V_2\cos\gamma_2\sin\phi_1 + \lambda_{h2}V_2\sin\gamma_2 + \lambda_{E1}\frac{V_2(T-D_2)}{mg} + 1 + k\cos^2\gamma_2 \tag{36}$$

where subscript '2' denotes slow time scale. Variables and (V_2, D_2) are current pursuer speed and drag.

The control variable in this time frame is γ_2. The optimality condition is

$$\frac{\partial H_2}{\partial\gamma_2} = 0; -\lambda_{x1}V_2\sin\gamma_2\cos\phi_1 - \lambda_{y1}V_2\sin\gamma_2\sin\phi_1 - \lambda_{h2}V_2\cos\gamma_2 - 2k\cos\gamma_2\sin\gamma_2 = 0 \tag{37}$$

After elimination of the Lagrange variables through Eqns. (23), (37) reduces to

$$\frac{V_2\sin\gamma_2(1+k)}{V_1(t_f)} + \lambda_{h2}V_2\cos\gamma_2 - 2k\cos\gamma_2\sin\gamma_2 = 0 \tag{38}$$

Therefore,

$$\lambda_{h2} = -\left[\frac{(1+k)}{V_1(t_f)} - \frac{2k\cos\gamma_2}{V_2}\right]\tan\gamma_2 \tag{39}$$

Additional condition for free final time $H_2(t) = 0$ and Eqn. (37) gives

$$-\frac{(1+k)V_2\cos\gamma_2}{V_1(t_f)} - \frac{(1+k)V_2\sin^2\gamma_2}{V_1(t_f)\cos\gamma_2} + 2k\sin^2\gamma_2 - \left\{\frac{(1+k)t_{go}}{V_1V_1(t_f)}\right\}\left\{\frac{V_2(T_{av}-D_2)}{m_{av}}\right\} + 1 + k\cos^2\gamma_2 = 0 \tag{40}$$

Which simplifies to

$$-\frac{(1+k)V_2}{V_1(t_f)\cos\gamma_2} + k\sin^2\gamma_2 = \left\{\frac{(1+k)t_{go}}{V_1V_1(t_f)}\right\}\left\{\frac{V_2(T_{av}-D_2)}{m_{av}}\right\} - (1+k) \tag{41}$$

Putting $\sin^2\gamma_2 = (1-\cos^2\gamma_2)$ and neglecting the cubic terms, from Eqn. (41) we get

$$\sec\gamma_2 = \left[\frac{(1+2k)}{1+k}\frac{V_1(t_f)}{V_2} - \frac{t_{go}(T_{av}-D_2)}{V_1 m_{av}}\right] \tag{42}$$

This equation gives the value of γ_2. Note that in Eqn. (42) V_1 is pursuer velocity at optimal altitude h_1, V_2 and D_2 are current pursuer speed and drag.

2.3.3 Fast Time Scale

(ϕ,γ) define the fast time scale. The Hamiltonian can be written as

$$H_3 = \lambda_{x1}V_2\cos\gamma_3\cos\phi_3 + \lambda_{y1}V_2\cos\gamma_2\sin\phi_1 + \lambda_{h2}V_2\sin\gamma_3 + \lambda_{E1}\frac{V_2(T-D_3)}{mg} + \lambda_{\phi3}\frac{g}{V_2}\frac{\eta_3\sin\sigma_3}{\cos\gamma_3} + \lambda_{\gamma3}\frac{g}{V_2} + 1 + k\eta_3^2 \tag{43}$$

where subscripts '3' denotes the variables in the fast time scale. I D_3 is the current drag of the pursuer.The original guidance problem control variables are (η_3,σ_3). The optimality condition is

$$\frac{\partial H_3}{\partial\eta_3} = \lambda_{\phi3}\frac{g}{V_2}\frac{\sin\sigma_3}{\cos\gamma_3} + \lambda_{\gamma3}\frac{g}{V_2}\cos\sigma_3 + \lambda_{E1}\frac{V_2}{mg}(-2\eta_3 D_{i3}) + 2\eta_3 k = 0 \tag{44}$$

where D_{i3} is the pursuer induced drag at current time. Other optimality condition $\frac{\partial H_3}{\partial\sigma_3} = 0$ Which yields

$$\lambda_{\phi3} = \lambda_{\gamma3}\tan\sigma_3\cos\gamma_3 \tag{45}$$

Eqns. (44) and (45) together give

$$\lambda_{\gamma3}\frac{g}{V_2}\frac{1}{\cos\sigma_3} = 2\left[\lambda_{E1}\frac{V_2 D_{i3}}{mg} - k\right]\eta_3 \tag{46}$$

Let us define

$$\Gamma = \left[\lambda_{E1}\frac{V_2 D_{i3}}{mg} - k\right] \tag{47}$$

where D_i is given in Eqn. (4). From Eqns. (45) and (46) we get

$$\lambda_{\gamma3} = 2\Gamma\frac{V_2}{g}\eta_3\cos\sigma_3;\ \lambda_{\phi3} = 2\Gamma\frac{V_2}{g}\eta_3\sin\sigma_3\cos\sigma_3 \tag{48}$$

Now, given current (γ_3, ϕ_3) and desired (optimal) (γ_2, ϕ_1) the orientation of the current velocity vector V_2 and the desired velocity vector have to be obtained. The direction cosine matrix (DCM) of the current and desired velocity vector are

$$C_i^c = \begin{bmatrix} \cos\gamma_3\cos\phi_3 & \cos\gamma_3\sin\phi_3 & \sin\gamma_3 \\ -\sin\phi_3 & \cos\phi_3 & 0 \\ -\sin\gamma_3\cos\phi_3 & -\sin\gamma_3\sin\phi_3 & \cos\gamma_3 \end{bmatrix}$$

$$C_i^d = \begin{bmatrix} \cos\gamma_2\cos\phi_1 & \cos\gamma_2\sin\phi_1 & \sin\gamma_2 \\ -\sin\phi_2 & \cos\phi_2 & 0 \\ -\sin\gamma_2\cos\phi_2 & -\sin\gamma_2\sin\phi_2 & \cos\gamma_2 \end{bmatrix} \tag{49}$$

Given the current and desired velocity vector (V_c, V_d), their corresponding direction cosines $(\hat{\upsilon}_c, \hat{\upsilon}_d)$, the turn angle (total angle through which flight path must be changed) is given by,

$$\cos\Delta\psi = \hat{\upsilon}_c\cdot\hat{\upsilon}_d = \cos\gamma_3\cos\gamma_2\cos(\phi_3-\phi_1) + \sin\gamma_3\sin\gamma_2 \tag{50}$$

Assuming the difference $(\phi_3-\phi_1)$ in the above Eqn. (50) to be very small yields

$$\cos\Delta\psi = \cos(\gamma_3-\gamma_2) \Rightarrow \Delta\psi = (\gamma_3-\gamma_2) \tag{51}$$

The lift vector is perpendicular to $\hat{\upsilon}_c$ and the optimal lift vector should be in the plane containing $(\hat{\upsilon}_c, \hat{\upsilon}_d)$. In Fig. 3 another coordinate system has been defined. Let this coordinate system have x' axis in the direction of the velocity vector of the pursuer, h' axis in the plane containing the h axis (Fig. 2) and the velocity vector V and perpendicular to V. The y' axis is defined automatically to complete the right handed coordinate system. Now referring to Eqn. (49) we transform the velocity in the desired frame (ϕ_1,γ_2) to the current velocity in the local vertical (LV) frame (ϕ_3,γ_3) as follows:

$$\vec{V}_{di} = \begin{bmatrix} V_{dxi} V_{dyi} V_{dzi} \end{bmatrix}^T = V_2\begin{bmatrix} \cos\gamma_2\cos\phi_1 & \cos\gamma_2\sin\phi_1 & \sin\gamma_2 \end{bmatrix}^T;$$

$$\vec{V}_c = C_i^c\vec{V}_{di} = \begin{bmatrix} V_{dx'} & V_{dy'} & V_{dz'} \end{bmatrix}^T \tag{52}$$

After some algebraic manipulations, we obtain,

$$V_{dy'} = V_2(-\sin\phi_3\cos\gamma_2\cos\phi_1 + \cos\phi_3\cos\gamma_2\sin\phi_1) \tag{53}$$

$$V_{dh'} = V_2(-\cos\phi_3\sin\gamma_3\cos\gamma_2\cos\phi_1 - \sin\phi_3\sin\gamma_3\cos\gamma_2\sin\phi_1 + \cos\gamma_3\sin\gamma_2)$$

Hence, the desired lift orientation angle in the current LOS plane is (Fig. 3)

$$\cos\sigma_3 - \frac{V_{dh'}}{\sqrt{V_{dy'}^2 + V_{dh'}^2}};\quad \sin\sigma_3 - \frac{V_{dy'}}{\sqrt{V_{dy'}^2 + V_{dh'}^2}} \tag{54}$$

Additional condition related to free terminal time $H_3(t)$=0 by assuming T and m to be T_{av} and m_{av} may be obtained using Eqn. (44) and the values of $(\lambda_{x1},\lambda_{y1},\lambda_{E1},\lambda_{h2},\lambda_{\phi3},\lambda_{\gamma3})$ as given in Eqns. (23), (25), (39) and (48). This condition is

$$-\frac{(1+k)V_2\cos\gamma_3}{V_1(t_f)} - \frac{(1+k)V_2\sin\gamma_2\sin\gamma_3}{V_1(t_f)\cos\gamma_2} + 2k\sin^2\gamma_2 - \frac{(1+k)t_{go}}{V_1V_1(t_f)}\frac{V_2(T_{av}-D_3)}{m_{av}} + 1 + k\eta_3^2 + 2\Gamma\eta_3^2\sin^2\sigma_3 + 2\Gamma\eta_3\cos\sigma_3(\eta_3\cos\sigma_3 - \cos\gamma_3) = 0 \tag{55}$$

From which

$$-\frac{(1+k)V_2\cos(\gamma_3-\gamma_2)}{\cos\gamma_2 V_1(t_f)} + 2k\sin^2\gamma_2 - \frac{(1+k)t_{go}}{V_1V_1(t_f)}\frac{V_2(T_{av}-D_3)}{m_{av}} + 1 + (k+2\Gamma)\eta_3^2 + 2\Gamma\eta_3\cos\sigma_3\cos\gamma_2 = 0 \tag{56}$$

Which, on simplification, using Eqn. (42) yields

$$(k+2\Gamma)\eta_3^2 - 2\Gamma\eta_3\cos\sigma_3\cos\gamma_2 + \frac{(1+k)V_2\sin^2(\gamma_3-\gamma_2)}{\cos\gamma_2 V_1(t_f)\cos(\gamma_3-\gamma_2)} + 2k\sin^2\gamma_2 - 2k = 0 \tag{57}$$

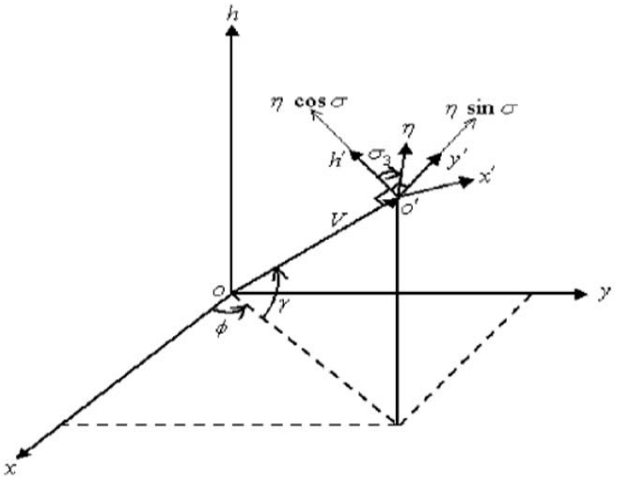

Figure 3. Coordinate transformation in context of SP guidance law.

Further simplification and approximation yields

$$(k+2\Gamma)\eta_3^2 - 2(\Gamma\cos\sigma_3\cos\gamma_2)\eta_3 - 2k\cos^2\gamma_2 + \frac{(1+k)V_2(\gamma_3-\gamma_2)^2}{\cos\gamma_2 V_1(t_f)} = 0 \quad (58)$$

Neglecting lower order terms and using Eqn. (51) the above equation yields the solution for η_3 as

$$\eta_3^2 = -\left[\frac{(1+k)V_2}{V_1(t_f)}\frac{\sec\gamma_2}{(k+2\Gamma)}\right](\Delta\psi)^2 \quad (59)$$

2.4 Boundary Layer Correction

Optimal altitude h_1 obtained by optimising cost function in Eqn. (32) issuboptimal because it does not satisfy boundary condition in Eqn. (6). So ad-hoc boundary-layer correction on optimal altitude[6, 11] h_1^* is given by

$$h_1^* = h_1\left(1-e^{-k_h r_h}\right) + h_f e^{-k_h r_h} \quad (60)$$

where, r_h is the horizontal range from pursuer to PIP and h_f is altitude of PIP. As suggested in[11]

$$k_h \in [0.00003, 0.03] \quad (61)$$

Ad-hoc boundary-layer correction on optimal γ_2 Eqn. (42) is given by[6, 11]

$$\gamma_2^* = k_\gamma\gamma_2 + (1-k_\gamma)\gamma_h \quad (62)$$

where, γ_2 is optimal pursuer flight path angle, γ_h is flight path angle of the PIP from the pursuer location and k_γ is a constant to satisfy[11]

$$k_h = \frac{(r-r_{see\,ker})}{(r_0-r_{see\,ker})}\varepsilon[0,1] \quad (63)$$

where r is the instantaneous distance from the pursuer to the evader, r_0 is distance from the pursuer to the evader at the start of the midcourse guidance and r_{seeker} is the seeker lock-on range. The schematic diagram of the SP based midcourse guidance law is shown in Fig. 4.

2.5 Computation of (T_{av}, m_{av})

Time varying Hamiltonian can be made H (t) = 0 by introducing average thrust and average mass.

$$T_{av} = \frac{1}{t_{go}}\int_t^{t_f} T(t)dt \;;\; m_{av} = \frac{1}{t_{go}}\int_t^{t_f} m(t)dt \quad (64)$$

where t is the current time and t_f is the predicted intercept time.

2.6 SP Algorithm for Midcourse Guidance

The analysis given above leads to the SP midcourse guidance algorithm which is given below.

Step 1: Define pursuer and evader initial conditions $(x_0, y_0, h_0, V_0, \phi_0, \gamma_0, x_{t0}, y_{t0}, h_{t0}, V_{t0}, \phi_{t0}, \gamma_{t0})$.

Step 2: If pursuer-evader distance is less than the seeker lock-on range, switch to terminal guidance.

Step 3: Calculate t_{go} and PIP (x_f, y_f, h_f).[15]

Step 4: Calculate optimal heading angle to the PIP, using Eqn. (20).

Step 5: Determine angle γ_h from pursuer to PIP. where $\gamma_h = \tan^{-1}\left[\frac{(h_f-h_0)}{d_h}\right]$. d_h is PIP-pursuer horizontal distance.

Step 6: Determine pursuer optimal altitude h_1 by optimising cost based on Eqns. (20), (32) and (33).

Step 7: h correction (boundary layer) $h_1^* = h_1\left(1-e^{-k_h r_h}\right) + h_f e^{-k_h r_h}$ where, $k_h \in [0.00003, 0.03]$

Step 8: Constraints h_1^* by $h_{\max}$ ((8)).Then, using Eqn. (34) obtain $V_1 = \sqrt{V^2 + 2g(h-h_1)}$.

Step 9: Determine the final value of V_1, i.e. $V_1(t_f)$ using Eqn. (26). $V_1(t_f) = V_1 + \frac{t_{go}(T_{av}-D_1)}{m_{av}}$

Step 10: Determine the flight path angle γ_2 using Eqn. (42).

Step 11: γ correction (boundary layer) $\gamma_2^* = k_\gamma\gamma_2 + (1-k_\gamma)\gamma_h$; $k_\gamma = \frac{(r-r_{see\,ker})}{(r_0-r_{see\,ker})}\varepsilon[0,1]$

Step 12: Determine σ_3 by comparing the desired and current pursuer velocity vector using Eqn. (54).

Step 13: Determine the load factor magnitude η_3 using Eqn. (59).

Step 14: Go to step 2 in the next guidance cycle.

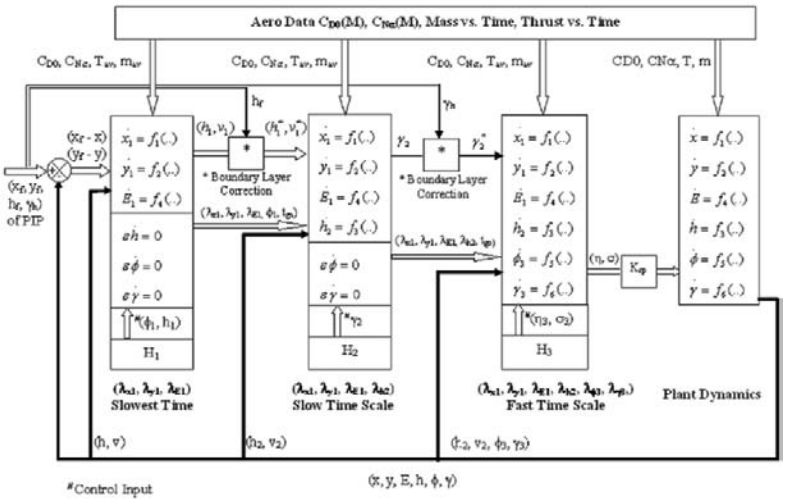

Figure 4. Schematic diagram of midcourse SP guidance law (equations for f_1…..f_6 are in Eqn. (1)).

3. 6DOF IMPLEMENTATION OF SP GUIDANCE ALGORITHM

The pursuer aerodynamic data base consisting of $C_{D0}(M,h)$ and $C_{N\alpha}$ used for this algorithm is shown in Fig. 5 and Fig. 6, respectively. The time history of the pursuer thrust and mass data for evaluation of (T_{av}, m_{av}) is given in Fig. 7. The output of SP guidance is (η_3, σ_3) along the pitch and pitch plane. These latax components are in local vertical frame. They have to be converted to body frame for generating autopilot. Demanded pursuer acceleration in local vertical frame transformed to body frame using latax demand.

$$\begin{bmatrix} a_{xd} & a_{yd} & a_{zd} \end{bmatrix}_B^T = C_i^b C_{l\upsilon}^i \begin{bmatrix} 0 & \eta_y & \eta_z \end{bmatrix}_{l\upsilon}^T \tag{65}$$

The pursuer position (x_m, y_m, z_m) and velocity (V_{xm}, V_{ym}, V_{zm}) are available from on-board strap-down internal navigation system (SDNIS). Its azimuth and elevation angles along with DCM, are

$$C_i^{l\upsilon} \begin{bmatrix} \cos\gamma_m \cos\phi_m & \cos\gamma_m \sin\phi_m & \sin\gamma_m \\ -\sin\phi_m & \cos\phi_m & 0 \\ -\sin\gamma_m \cos\phi_m & -\sin\gamma_m \sin\phi_m & \cos\gamma_m \end{bmatrix}$$

$$\phi_m = \tan^{-1}\left(V_{ym}/V_{xm}\right); \gamma_m = \tan^{-1}\left(V_{zm}\sqrt{V_{xm}^2 + \hat{V}_{xm}^2}\right) \tag{66}$$

Calculation of total drag using Eqn. (4) is very important for computation of optimal altitude. So, latax achieved by the pursuer and sensed by the accelerometer is fed to the SP guidance block for accurate induced drag calculation. Let (η_{yf}, η_{zf}) be the fed back latax components in the local vertical frame from the acceleration output after necessary orthogonal transformations. The transformation equations are

$$\begin{bmatrix} \eta_{xf} \\ \eta_{yf} \\ \eta_{zf} \end{bmatrix}_{l\upsilon} = C_i^{l\upsilon} C_b^i \begin{bmatrix} a_x \\ a_y \\ a_y \end{bmatrix}_{sensed}$$

$$\eta_f = \sqrt{\eta_{yf}^2 + \eta_{zf}^2}; D = D_0 + D_i \eta_f^2; D_0 = C_{D0} QS; D_i = \frac{m^2 g^2 k_d}{QS}, k_d = \frac{1}{C_{N\alpha}} \tag{67}$$

Input to SP algorithm is $(x_m, y_m, z_m, V_{xm}, V_{ym}, V_{zm})$ obtained from the SDNIS. An EKF based on board radar estimator is used to process the noisy range, azimuth and elevation of evader to estimate its position and velocity components relative to the aircraft. The estimated inertial position and velocity components of evader is sent to the pursuer through a data link at a certain frequency. Position and velocity information of both pursuer and evader arev input to the SP algorithm which generates (η_y, η_z) as guidance output.

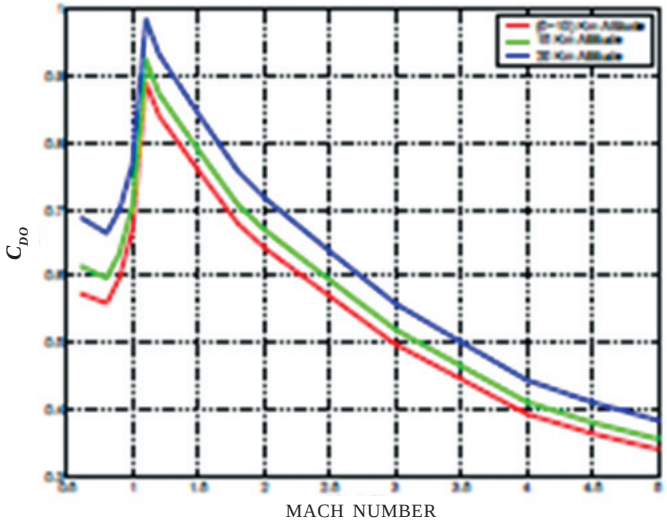

Figure 5. Pursuer C_{DO} variation with Mach number and altitude.

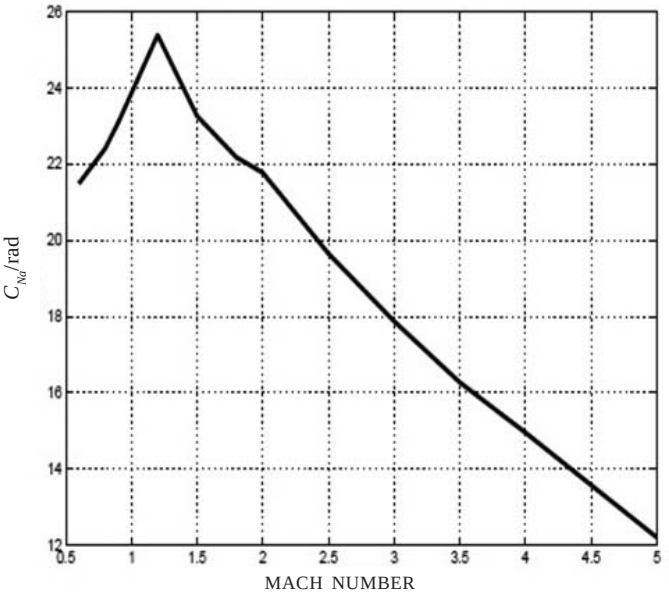

Figure 6. Pursuer C_{Na} variation with Mach number.

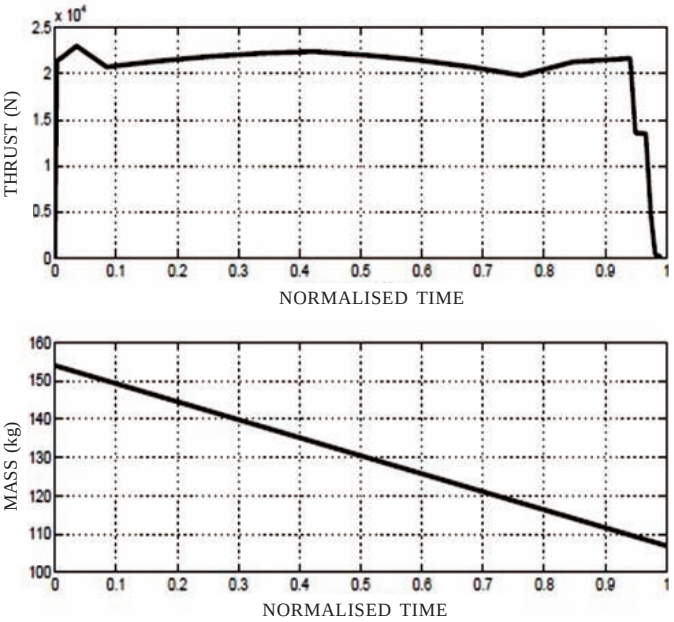

Figure 7. Time history of pursuer thrust and mass.

One important practical constraint in midcourse guidance is that the pursuer has to be always within the data link beam width of $\pm 20^0$ with respect to the launch aircraft for receiving the evader information (Fig. 2). So at any time instant based on data link maximum look angle constraint, launch aircraft and pursuer SDNIS information, $h_{\max}$ (Section 2.6) was computed online. Calculation of the h_1 based on its constraints $h_{\max}$ (8) has been carried out in the guidance algorithm. Instantaneous

position (x_a, y_a, z_a) and velocity components (V_{xa}, V_{ya}, V_{za}) of the aircraft are available from aircraft SDINS. At any time instant the pursuer LOS with respect to the aircraft can be written as

$$\Delta x = x_m - x_a; \quad \Delta y = y_m - y_a; \quad \Delta h = h_m - h_a;$$

$$\phi_{lma} = \tan^{-1}(\Delta x/\Delta y); \; \gamma_{lma} = \tan^{-1}\left(\Delta h/\sqrt{\Delta x^2 + \Delta y^2}\right) \quad (68)$$

The pursuer LOS as given in Eqn. (68) has to be always within $\gamma_{lma}^{\max} = \pm 20^0$ during midcourseguidance and

$$h_{\max} = \sqrt{(x_m - x_a)^2 + (y_m - y_a)^2}\,\tan\gamma_{lma}^{mxa} + z_a \quad (69)$$

Demanded pursuer optimisation altitude from Eqn. (32) is modified as $h_1 = \min(h_{\max}, h_1)$ and used in Eqn. (34).

4. 6DOF SIMULATION RESULTS

Here we show through simulation that the SP guidance law during midcourse gives rise to more closing velocity at the end of midcourse which in turn gives more launch range when compared to PN guidance. First we will consider a typical engagement (Table 1) with a non-manoeuvring evader. For this case study PN or SP was used during the midcourse phase and PN was used during terminal homing phase. The aerodynamic data, the purser mass history and thrust profile have been discussed previously. After launch from the launch aircraft, the pursuer's initial elevation and azimuth is kept constant for 2.5 s using an altitude hold autopilot. Also, at launch, the on-board radar estimator of the launch aircraft is initialised to process the evader noisy measurements, tracked by on-board radar. After attitude hold phase, the midcourse guidance is initiated. During this period, the evader position and velocity components estimated by the radar EKF, are up-linked to the pursuer through data link from the launch aircraft. Once the pursuer-evader range becomes less than 15 km, the pursuer on-board seeker starts tracking the evader. At this time instant. EKF based seeker estimator is initialised to estimate the relative position and velocity components of evader with respect to pursuer by processing the noisy seeker measurements. At 10 km range-to-go the radar based midcourse guidance ends and PN based terminal homing guidance starts. From this time onwards the pursuer is in autonomous mode and seeker based estimator output is used by the terminal PN guidance for pursuer latax generation. During midcourse guidance, radar EKF sampling as well as update of position and velocity information of evader to pursuer is carried out at every 100 ms using the data link. During terminal guidance, seeker EKF processes seeker measurements at 10 ms interval. Guidance update during midcourse, as well as during the terminal phase, is carried out at 10 ms interval.

Table 1. Typical engagement scenario for SP midcourse guidance (Non manoeuvring evader)

Head-on engagement, Seeker lock-on range = 10 km		
Parameter	**Pursuer**	**Evader**
Initial velocity	380 m/s (M = 1.2)	228 m/s (M = 0.7)
Initial elevation angle	0 deg.	0 deg.
Initial azimuth angle	0 deg.	180 deg.
Initial altitude	8 km	6 km

Details of evader model, PN guidance law and terminal seeker estimator are given in Srinivasan[16], *et al.* A brief description of midcourse radar estimator in launch aircraft is given in Appendix A. In 6DOF simulation the guidance law operates in the presence of sensor noise, body rate coupling with LOS rates of seeker, estimation error, guidance lag, autopilot lag and actuator dynamics. Three loop autopilot[17] has been used in simulation for tracking guidance demanded latax along both yaw and pitch plane. The control surface deflection demands are passed through four independent actuators. The actuators have been modelled as a second order system with command input/output transfer function $\left\|\dfrac{\delta_0}{\delta_i} = \dfrac{\omega_a^2}{s^2 + 2\zeta_a\omega_a s + \omega_a^2}\right\|$ with ζ_a = 0.366, ω_a = 20 Hz, $\delta_{\max}$ =24 deg. and $\dot{\delta}_{\max}$ =25. deg/s. The actuator nonlinearities consist of dead zone and backlash of 0.23 deg and 0.115 deg half-width respectively. Based on the simulation results we infer the following:

(a) Using PN guidance during midcourse, maximum launch range is 41km with impact Mach 1.1

(b) Using SP guidance with maximum range of 48 km can be achieved for the same initial condition as in PN. During midcourse phase maximum LOS with respect to launch aircraft is 19 deg which is within data link limit. In this case interception Mach number is 1.2.

(c) Pursuer velocity and Mach number corresponding to PN guided trajectory (41 km launch range) and SP guided trajectory (48 km launch range) are shown in Fig. 8. Time variation of pursuer LOS with respect to aircraft $(\phi_{lma}, \gamma_{lma})$ along yaw and pitch plane are shown in Fig. 9. Complete engagement trajectory for all the above cases is shown in Fig. 10.

(d) The demanded and achieved *t* achieved accelerations in pitch and yaw planes along the body frame corresponding to SP during midcourse and PN during terminal homing are shown in Fig. 11. From the figure we see that initially pursuer experiences high latax to reach the optimal altitude which is the main reason for pitch up.

A complete 6 DOF Monte Carlo simulation of the given engagement condition (case study of Table 1) has been carried out to study robustness of the present SP guidance law in the presence of uncertainty in the initial kinematic conditions aero data thrust wing/fin misalignment angles, centre of gravity (CG), mass moment of inertia (MMI) of pursuer and random noise sequence in airborne radar and pursuer seeker measurements. Variation on different parameters for MC simulation is given in Table 2 which are based on experiments and wind tunnel tests and other subsystem consideration. MC engagement result corresponding to both (PN+PN) and (SP+PN) as (midcourse + terminal) guidance law for 41 km and 48 km lock on range is given in Table 3. The results are based on 100 runs. From the results we can infer that for a given engagement condition, subjected to data link hardware constraint it is possible to increase the launch range by 17 per cent through SP midcourse guidance law over PN for supersonic interception. Supersonic interception is preferred for overall system effectiveness and lethality point of view. Cumulative distribution frequency (CDF) comparison of miss distance corresponding to PN and SP midcourse guidance law is shown in Fig. 12.

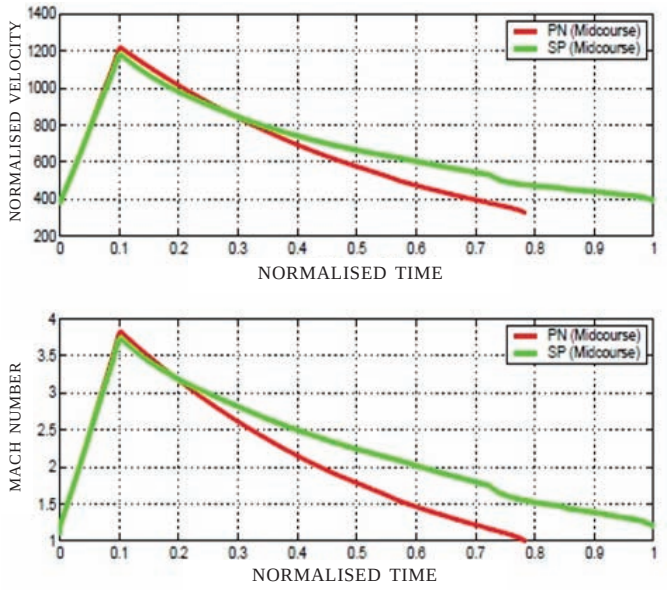

Figure 8. Time history of pursuer velocity and match number (PN or SP during midcourse, PN during terminal phase).

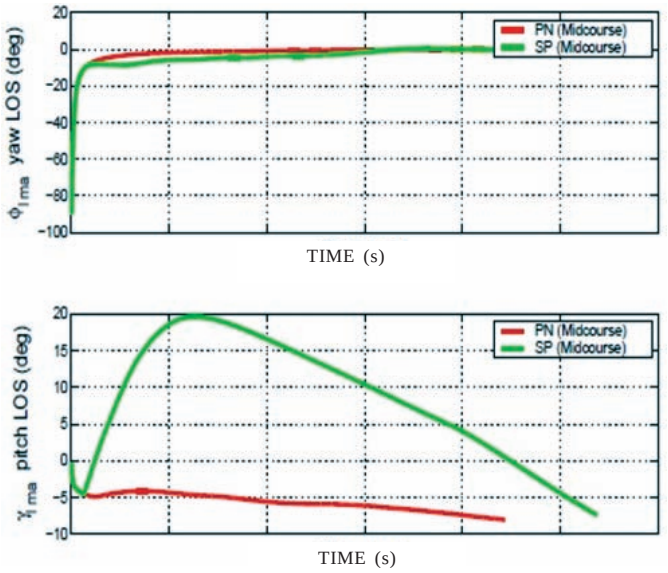

Figure 9. Time history of ($\phi lma, \gamma l\, ma$) (PN or SP during midcourse, PN during terminal phase).

We next obtain the outer launch boundary for engagement at 10 km altitude corresponding to anon-manoeuvring evader. The inputs for launch boundary generation are seeker lock on-range = 10 km, pursuer and evader initial velocity = 370 m/s (M = 1.2), their initial elevation = 0 deg, pursuer initial azimuth = 0 deg. and evader initial azimuth ε (0, 180) deg. With these initial conditions, the normalised outer launch envelope using PN and SP as midcourse guidance is shown in Fig.13. With the present data link constraint it is possible to extend range by about 15 km for engagements at 10 km altitude.

5. CONCLUSIONS

In this study SP guidance algorithm originally developed by Sridhar[3], *et al.* and Cheng[5], *et al.* has been derived and thoroughly analysed. The guidance law has been implemented

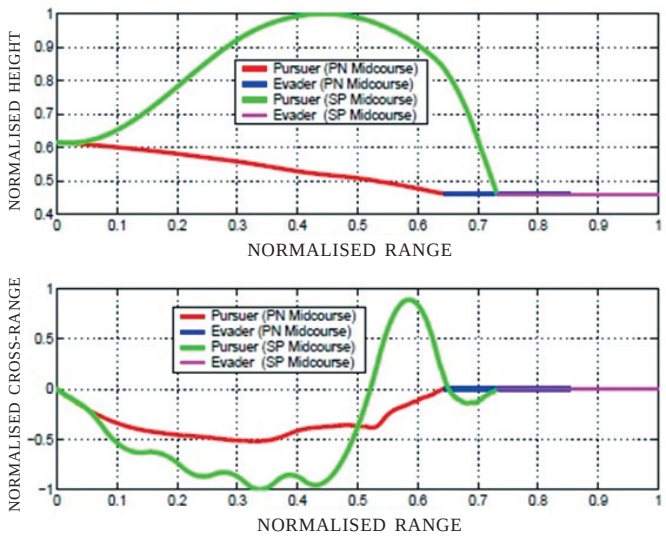

Figure 10. Engagement trajectory of pursuer and evader.

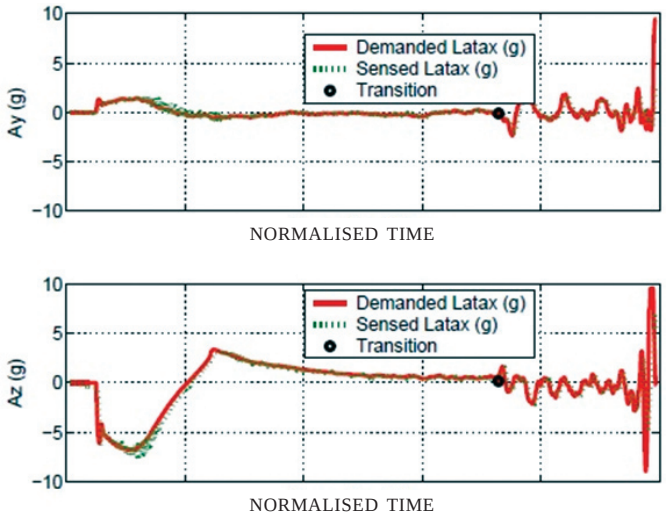

Figure 11. Demanded and achieved latex (η_y, η_p) of pursuer in body frame (SP during midcourse, PN during terminal phase).

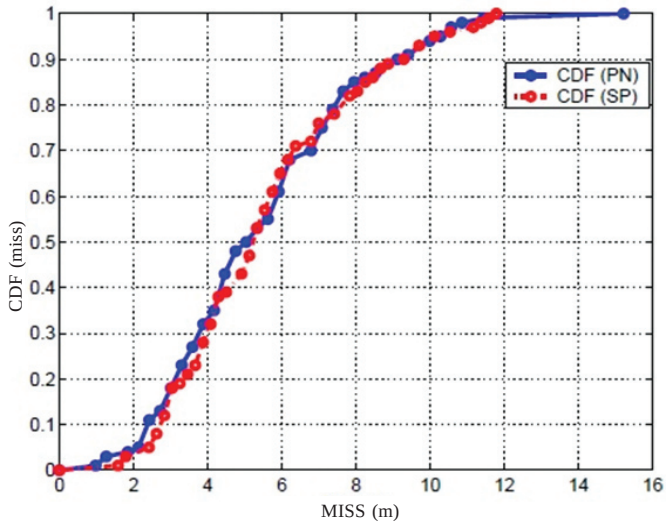

Figure 12. Comparison of cumulative distribution function of miss distance (PN or SP for midcourse, PN during terminal phase).

Table 2. Perturbation of different parameters in 6 DOF simulation for MC Study of Table1

Parameters	Distribution type*		Factor**	Parameters	Distribution type*		Factor**
$t_i(s)$	UD	(0.2, 0.3)	AFZ	Thrust (s)	UD	(6.7, 7.3)	AFN
$u_i(m/s)$	UD	(370, 390)	AFZ	Pitch misalignment (°)	ND	(0, 0.2)	AFN
$\upsilon_i(m/s)$	UD	(-2, 2)	AFZ	Yaw misalignment (°)	ND	(0, 0.2)	AFN
$w_i(m/s)\upsilon$	UD	(-5, 5)	AFZ	Wing misalignment (°)	ND	(0, 0.2)	AFN
p_i(°/s)	UD	(-2, 2)	AFZ	Fin misalignment (°)	ND	(0, 0.2)	AFN
q_i(°/s)	UD	(-2, 2)	AFZ	I_{xx} (kg m^2)	UD	(-0.1, 0.1)	AFN
r_i(°/s)	UD	(-2, 2)	AFZ	I_{yy} (kg m^2)	UD	(-1.0, 1.0)	AFN
ψ(°)	UD	(-2, 2)	AFZ	I_{zz} (kg m^2)	UD	(-1.0, 1.0)	AFN
θ(°)	UD	(-10, -2)	AFZ	C_x	ND	(0, 0.15)	AFN
ϕ(°)	UD	(-2, 2)	AFZ	C_N	ND	(0, 0.15)	AFN
mass (kg)	UD	(-3, 3)	AFZ	C_M	ND	(0, 0.15)	AFN
x-cg (mm)	UD	(-3, 3)	AFZ	C_l	ND	(0, 0.15)	AFN
y-cg (mm)	UD	(-2, 2)	AFZ	C_n^{δ}	ND	(0, 0.15)	AFN
z-cg (mm)	UD	(-2, 2)	AFZ	C_m^{δ}	ND	(0, 0.15)	AFN
h (km)	UD	(-0.5, 0.5)	AFZ				

*ND=Normal Distribution with $(\mu, 3\sigma)$, UD=Uniform distribution with (lower, upper) bound
**AFN=Additive factor over nominal value, AFZ=Additive factor over zero

Table 3. MC based 6 DOF simulation results of engagement of Table 1

	Midcourse end*			Terminal impact			
(Mid + Term) guidance	Time (s)	Altitude (km)	Mach	Time (s)	M_{impact}	Estimated miss (m)	True miss (m)
PN + PN	(28.4 ± 0.74)	(6.6 ± 0.05)	(1.86 ± 0.15)	(42.1 ± 1.6)	(1.22 ± 0.15)	(5.1 ± 2.5)	(5.6 ± 2.4)
SP + SP	(36.6 ± 1.03)	(8.87 ± 0.07)	(1.90 ± 0.14)	(50.02 ± 1.8)	(1.40± 0.14)	(5.2 ± 2.2)	(5.6 ± 2.6)

*The MC results are normally distribution with

in realistic 6 DOF simulations model of an air-to-air engagement in the presence of sensor noise, autopilot lag and actuator nonlinearities. The paper has proposed an improved SP based algorithm from the point of view of practical on board implementation. Based on the Monte Carlo based 6 DOF simulation studies it is inferred that SP guidance is a viable alternate to PN guidance for midcourse application within the constraint of maximum look angle of the launch aircraft. Guidance gain tuning may be explored for better robustness of SP guidance algorithm[10, 18] as avenues for further research over the present work.

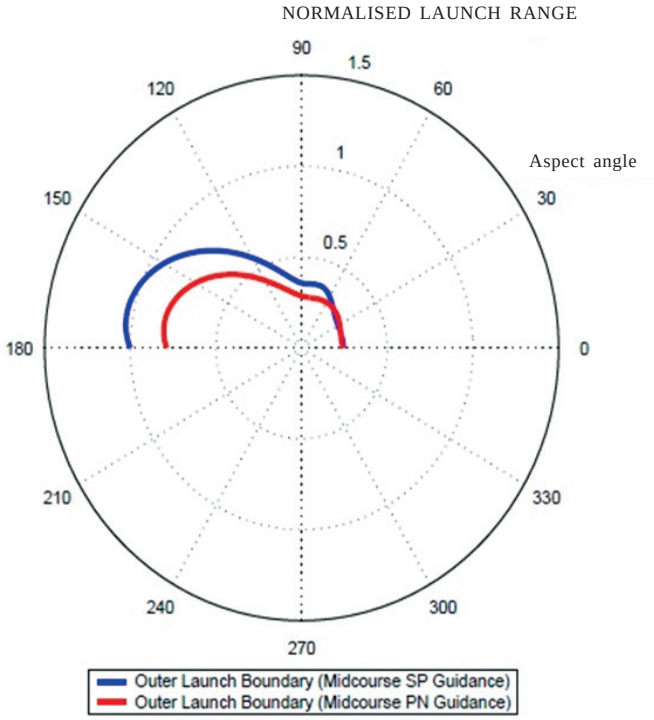

Figure 13. Comparison of normalised launch boundary with SP and PN as midcourse guidance law (10 km altitude).

REFERENCES

1. Bryson, A. & Ho, Y.C. Applied optimal control. Hemisphere publication, Washington DC, 1969.
2. Naidu, D.S. & Calise, A.J. Singular perturbation and time scales in guidance and control of aerospace system: A survey. *J. Guidance, Control Dynamics*, 2001, **24**(6), 1057-1078. doi : 10.2514/2.4830
3. Robert, E. & O'Malley. Historical development in singular perturbations. Springer International Publishing, Switzerland, 2014
4. Sridhar, B. & Gupta, N.K. Missile guidance law based on singular perturbation methodology. *J. Guidance, Control Dynamics*, 1980, **3**(2), 158-165.doi : 10.2514/3.55964
5. Calise, A.J. Singular perturbation techniques for on-line optimal flight path control. *J. Guidance, Control Dynamics*,

1981, **4**(4), 398-405. doi : 10.2514/3.56092
6. Cheng, V.H.L. & Gupta, N.K. Advanced midcourse guidance for air-to-air missiles. *J. Guidance, Control Dynamics*, 1986, **9**(2), 135-142. doi : 10.2514/3.20081
7. Sheu, D.; Vinh, N.X. & Howe, R.M. Application of singular perturbation methods for three-dimensional minimum time interception. *J. Guidance, Control Dynamics*, 1991, **14**(2), 360-367. doi : 10.2514/3.20647
8. Weston, A.; Cliff, G. & Kelley, H. On-board near optimal climb-dash energy management. *J. Guidance, Control Dynamics*, 1985, **8**(3), 321-325. doi : 10.2514/3.19982
9. Menon, P.K.A. & Briggs, M.M. Near-optimal midcourse guidance for air-to-air missiles. *J. Guidance, Control Dynamics*, 1990, **13**(4), 596-602. doi : 10.2514/3.25375
10. Kee, P.E.; Dong, L. & Siong, C.J. Near optimal midcourse guidance law for flight vehicle. *In* Proceedings of 36th Aerospace Science Meeting and Exhibit, Reno, NV, January 1998. Paper No. AIAA-98-0583-CP. doi : 10.2514/6.1998-583
11. Raikwar, A.G.; Ghose, D.; Swamy, K.N. & Bhat, M.S. Design, evaluation of a midcourse guidance law for a BVRAAM. Indian Institute of Sciences, Bangalore, India, August 1997. Technical Report No. JATP-97-001,
12. Erez, Sigal & Joseph, Z. Ben-Asher. Near-optimal missile guidance with pulse motor control logic. *In* Proceedings of AIAA Guidance, Navigation and Control Conference and Exhibit, 2-5 August 2010, Toronto, Ontario, Canada, August 2010. Paper No. AIAA-2010-8055-CP.
13. Chandrakanth, Annam. Midcourse guidance of air to surface missiles. Department of Aerospace Engineering, IISc, Bangalore, India, June 2015. ME Thesis.
14. Fossard, A.J. & Normand-Cyrot, D. Nonlinear systems. volume 3. Chapman and Hall, UK, 1997. doi: 10.1007/978-1-4615-6395-2
15. Srivastava, R; Sarkar, A.K.; Ghose, D. & Gollakota, S. Nonlinear three dimensional composite guidance law based on feedback linearisation. *In* Proceedings of AIAA Guidance, Navigation and Control Conference and Exhibit, Providence, Rhode Island, August 2004. Paper No. AIAA-2004-4903-CP. doi : 10.2514/6.2004-4903
16. Sarkar, A.K.; Ananthasayanam, M.R.; Srinivasan, T. & Kar, P.K. Performance study of radar and seeker estimator in a realistic tactical scenario. *J. Guidance, Control Dynamics*, 2009, **32**(6), 1912-1920. doi : 10.2514/6.2008-7462
17. Zarchan, P. Tactical and strategic missile guidance. AIAA Inc., Ed.4th, 2002.
18. Kokotovic, V.P.; Khalil, H.K. & O'Reilly, J. Singular perturbation methods in control: Analysis and design. Academic Press Inc. (London), 1986.

CONTRIBUTORS

MR M Manickavasagam had the BE (Aeronautical Engineering) from MIT (Anna University) and ME (Aerospace Engineering) from IISc Bengaluru. He has been working as scientist in Advance System Laboratory, Hyderabad. His current research interest are : System design for long range flight vehicle, simulation and modelling, trajectory optimisation and multi-disciplinary design optimisation for flight vehicle.

Mr A.K. Sarkar had BE (Aeronautical Engineering) from IIT Kharagpur and ME (Computer Science) from IIT Madras and currently pursuing his PhD from IISc Bengaluru. Presently working as scientist in Defence Research and Development Laboratory, Hyderabad. His research interests are : Fight mechanics, guidance and optimisation techniques for flight vehicle system design.

Dr V. Vaithiyanathan is associate dean and professor of school of computing in SASTRA.

APPENDIX

A. EKF Based Aircraft Radar Estimator during Midcourse Phase

Launch aircraft radar measures evader position relative to itself $(\Delta x_t, \Delta y_t, \Delta z_t)$ in the polar form as

$$\Delta r_t = \sqrt{\Delta x_t^2 + \Delta y_t^2 + \Delta z_t^2};\ \Delta a_t = \tan^{-1}\frac{\Delta y_t}{\Delta x_t}\ \Delta e_t = \tan^{-1}\frac{\Delta z_t}{\sqrt{\Delta x_t^2 + \Delta y_t^2}} \tag{70}$$

These measurements are contaminated by a zero mean Gaussian noise given by η_r, η_α and η_e as

$$\Delta r_m = \Delta r_t + \eta_r;\ \Delta a_m = \Delta a_t + \eta_\alpha;\ \Delta e_m = \Delta e_t + \eta_e; \tag{71}$$

Realistic radar measurements noise covariance R_p for $(\Delta r_m, \Delta a_m, \Delta e_m)$ as $(10000m^2, 4\times10^{-2}\deg^2, 4\times10^{2}\deg^2)$ have been taken. The converted measurements in Cartesian Coordinateare

$$\Delta x_{tm} = \Delta r_m \cos\Delta e_m \cos\Delta a_m;\ \ \Delta y_{tm} = \Delta r_m \cos\Delta e_m \sin\Delta a_m;$$
$$\Delta z_{tm} = \Delta r_m \sin\Delta a_m \tag{72}$$

EKF based radar estimator[16] has been used to estimate position and velocity components of evader relative to aircraft $(\Delta\hat{x}_t, \Delta\hat{y}_t, \Delta\hat{z}_t, \Delta\hat{V}_{xt}, \Delta\hat{V}_{\dot{y}t}, \Delta\hat{V}_{zt})$ based on the measurements given in (72). Evader position and velocity components in the inertial frame are obtained by algebraically adding aircraft position and velocity components available from its SDNIS and transmitted to pursuer through data link as follows:

$$\hat{x}_t = x_a + \Delta\hat{x}_t;\ \hat{y}_t = y_a + \Delta\hat{y}_t;\ \hat{z}_t = z_a + \Delta\hat{z}_t$$
$$\hat{V}_{xt} = V_{xa} + \Delta\hat{V}_{xt};\ \hat{V}_{\dot{y}t} = V_{ya} + \Delta\hat{V}_{\dot{y}t};\ \hat{V}_{zt} = V_{za} + \Delta\hat{V}_{zt} \tag{73}$$